WATER RESOURCES RESEARCH, VOL. 30, NO. 4, PAGES 1153–1171, APRIL 1994

A physically based model for the topographic control on shallow landsliding

David R. Montgomery
Department of Geological Sciences and Quaternary Research Center, University of Washington, Seattle

William E. Dietrich
Department of Geology and Geophysics, University of California, Berkeley

Abstract. A model for the topographic influence on shallow landslide initiation is developed by coupling digital terrain data with near-surface through flow and slope stability models. The hydrologic model TOPOG (O'Loughlin, 1986) predicts the degree of soil saturation in response to a steady state rainfall for topographic elements defined by the intersection of contours and flow tube boundaries. The slope stability component uses this relative soil saturation to analyze the stability of each topographic element for the case of cohesionless soils of spatially constant thickness and saturated conductivity. The steady state rainfall predicted to cause instability in each topographic element provides a measure of the relative potential for shallow landsliding. The spatial distribution of critical rainfall values is compared with landslide locations mapped from aerial photographs and in the field for three study basins where high-resolution digital elevation data are available: Tennessee Valley in Marin County, California; Mettman Ridge in the Oregon Coast Range; and Split Creek on the Olympic Peninsula, Washington. Model predictions in each of these areas are consistent with spatial patterns of observed landslide scars, although hydrologic complexities not accounted for in the model (e.g., spatial variability of soil properties and bedrock flow) control specific sites and timing of debris flow initiation within areas of similar topographic control.

Introduction

The spatial and temporal distribution of shallow landsliding are important controls on landscape evolution and a major component of both natural and management-related disturbance regimes in mountain drainage basins [e.g., *Hack and Goodlet*, 1960; *Dietrich and Dunne*, 1978; *Tsukamoto et al.*, 1982; *Okunishi and Iida*, 1983; *Dietrich et al.*, 1986; *Benda and Dunne*, 1987; *Crozier et al.*, 1990]. The sudden failure and high speed of shallow landslides that mobilize as debris flows make them particularly destructive to downstream resources, property, and lives [e.g., *Smith and Hart*, 1982; *Ellen and Wieczorek*, 1988; *Brabb and Harrod*, 1989]. Debris flows may also scour steep channels to bedrock and accelerate sediment delivery to downstream, lower-gradient channels. Increasing pressure to use upland landscapes and concurrently to minimize downstream impacts necessitates development of objective methods for assessing the distribution of potential debris flow source areas and run out paths.

Debris flows typically occur during intense storms or periods of extended rainfall [e.g., *Caine*, 1980], reflecting the effect of elevated soil moisture on soil strength. Topography influences shallow landslide initiation through both concentration of subsurface flow and the effect of gradient on slope stability. Other factors that also influence the spatial and temporal distribution of shallow landsliding include soil thickness, conductivity, and strength properties; rainfall intensity and duration; subsurface flow orientation; bedrock fracture flow; and root strength. While these factors are important controls, their spatial distribution are difficult to determine. On the other hand, most studies report that shallow landslides only become important above a threshold hillslope gradient and that these landslides most commonly originate in areas of topographic convergence [e.g., *Campbell*, 1975; *Reneau and Dietrich*, 1987a; *Ellen et al.*, 1988].

In this paper, we present a quantitative model for assessing the topographic influence on shallow landsliding. Models for the generation of soil saturation and slope instability are combined with digital terrain data to predict the steady state rainfall necessary for slope failure throughout a catchment. Our primary assumption here is that while local properties surely affect the timing, size, and behavior of a shallow landslide, the dominant control on where they occur is the local surface topography, as it in turn defines local slope and shallow subsurface flow convergence. The relative simplicity of the model is attractive for the typical case where little is known about the spatial variability of the other important factors that affect slope stability. The coupled model delineates areas of the landscape with similar topographic control on shallow landslide initiation.

Previous Work

There are many approaches to assessing landslide hazards. The most widely used techniques include (1) field inspection using a check list to identify sites susceptible to

Paper number 93WR02979.
0043-1397/94/93WR-02979$05.00

landsliding [e.g., *Neely and Rice*, 1990]; (2) projection of future patterns of instability from analysis of landslide inventories [e.g., *Wright et al.*, 1974; *DeGraff*, 1985; *Degraff and Canuti*, 1988]; (3) multivariate analysis of factors characterizing observed sites of slope instability [e.g., *Neuland*, 1976, 1980; *Carrara et al.*, 1977; *Carrara*, 1983; *Roth*, 1982; *Pike*, 1988; *Mark*, 1992]; (4) stability ranking based on criteria such as slope, lithology, land form, or geologic structure [e.g., *Brabb et al.*, 1972; *Campbell*, 1975; *Hollingsworth and Kovacs*, 1981; *Fowler*, 1984; *Reneau and Dietrich*, 1987b; *Smith*, 1988; *Seely and West*, 1990; *Montgomery et al.*, 1991]; and (5) failure probability analysis based on slope stability models with stochastic hydrologic simulations [e.g., *Burroughs*, 1984; *Burroughs et al.*, 1985; *Dunne*, 1991; *Hammond et al.*, 1992; *Sidle*, 1992]. Each of these approaches is valuable for certain applications. None, however, takes full advantage of the fact that debris flow source areas are, in general, strongly controlled by surface topography through shallow subsurface flow convergence, increased soil saturation, and shear strength reduction. This topographic influence on near-surface hydrologic response, and thus debris flow generation, can be modeled using digital elevation data.

Two approaches have been proposed recently that use digital terrain data to represent spatial distributions of slope instability. One involves generating topographic attributes from digital elevation data (e.g., slope) which can be combined with other characteristics such as vegetation, or lithology, in a geographical information system (GIS) to identify hazardous areas based on observed correlations between landsliding and these attributes [*Carrera et al.*, 1991]. While this approach may provide an effective method for identifying areas in which debris flows are an important process, it tends to classify relatively large areas into stability types, rather than resolve fine-scale patterns of instability that would be particularly valuable for hazard assessment or land management. Moreover, such models tend to be site specific because of the empirical basis of GIS-based multivariate analysis.

The other approach is to use digital elevation data to make more process-based predictions of site instability. Okimura and colleagues [*Okimura and Ichikawa*, 1985; *Okimura and Nakagawa*, 1988] used a grid-based digital elevation model in a finite difference model of shallow subsurface flow under steady rainfall. Predicted pore pressure values were used to calculate the stability of individual grid cells using a form of the infinite slope model. Most of the scars in a small (0.1 km^2) study catchment were correctly identified by their model, although many more cells were predicted to be unstable than were actually observed.

Here we build upon this approach and our previous work [*Dietrich et al.*, 1992, 1993] to explore the utility of a process-based slope stability model to predict the location of shallow landslides in three catchments in the coastal mountains of the western United States. We combine a contour-based steady state hydrologic model with a simple slope stability model and reduce this coupled model to its most essential components. The steady state assumption allows isolation of the topographic influence on debris flow initiation and thus development of a process-based relative hazard map. The simplicity of our model is consistent with the lack of detailed knowledge one can expect to acquire about the spatial variability of soil thickness, strength, and hydrologic properties. We have also added a debris flow routing and deposition algorithm that enhances the usefulness of our model in linking hillslope instability with downslope consequences.

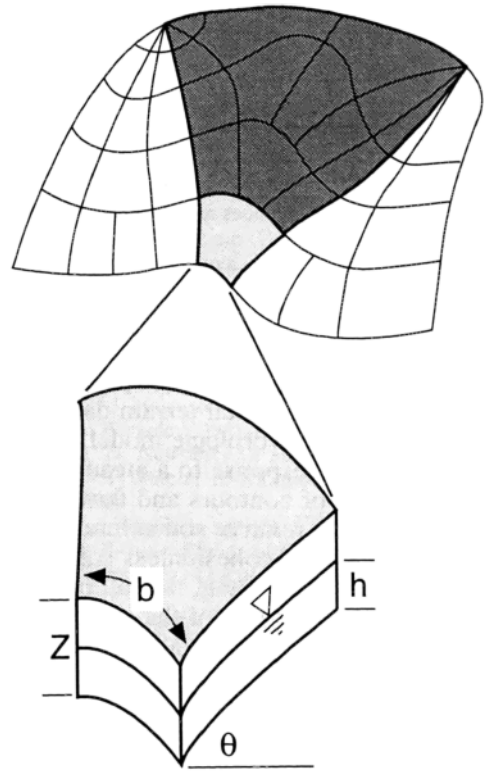

Figure 1. Topographic elements used in the program TOPOG [*O'Loughlin*, 1986] are defined by the intersections of contours (gray lines) and flow tube boundaries (black lines). The upslope contributing area a (shaded) is the cumulative drainage area of all topographic elements draining into an element. Definitions of other parameters used in the analysis are illustrated in the bottom part of the figure.

Model

In our application the hydrologic model, TOPOG [*O'Loughlin*, 1986], uses a steady state rainfall and maps the spatial pattern of equilibrium soil saturation based on analysis of upslope contributing areas, soil transmissivity, and local slope (Figure 1). The model divides a catchment into topographic elements defined by the intersection of contours and flow tube boundaries orthogonal to contours. The net rainfall (precipitation less evapotranspiration and deep drainage into bedrock) becomes shallow subsurface flow, which is routed down flow tubes, allowing calculation of the local flux through each topographic element. The hydrologic model thus reduces to a calculation of wetness W, which is the ratio of local flux at a given steady state rainfall to that at soil profile saturation:

$$W = qa/bT \sin \theta \quad (1)$$

in which q is the net rainfall rate, a is the contributing area draining across b the contour length of the lower bound to each element, T is soil transmissivity when saturated, and θ is the local slope (in degrees) of the ground surface (Figure

1). When wetness exceeds 1.0, the ground experiences saturation overland flow. If we assume that the saturated conductivity does not vary with depth beneath the surface, then we can write $T = Kz \cos \theta$ and (1) can be simplified for the case where $W \leq 1.0$ to

$$W = K \sin \theta h \cos \theta / K \sin \theta z \cos \theta = h/z \quad (2)$$

where K is the saturated conductivity of the soil, h is the thickness of saturated soil, and z is the total soil thickness [*Dietrich et al.*, 1993]. This simplification allows us to write the infinite slope stability model for cohesionless soils (with a wet bulk density of ρ_s relative to the bulk density of water ρ_w) and slope-parallel seepage as either

$$\tan \theta = [1 - W(\rho_w/\rho_s)] \tan \phi \quad (3a)$$

or

$$W = (\rho_s/\rho_w)[1 - (\tan \theta/\tan \phi)]. \quad (3b)$$

In (3a), wetness would be calculated from (1) and if $W > 1.0$, then W is set equal to 1.0, as the remaining water runs off as overland flow. Substitution of (1) into (3b) allows this failure criterion to be expressed in terms of drainage area per unit contour length. Thus topographic elements, where

$$a/b \geq (T/q) \sin \theta (\rho_s/\rho_w)[1 - (\tan \theta/\tan \phi)] \quad (4)$$

are predicted to be unstable. In this form, the topographic variables (a/b, $\sin \theta$, and $\tan \theta$), hydrologic variables (T, q), and soil variables ($\tan \phi$ and ρ_s) are clearly defined. Our model does not explicitly state that soil depth is spatially constant, but the assumptions of a constant transmissivity and that saturated conductivity does not vary with soil depth are most easily accomplished if this is the case. In essence, our model holds all soil properties constant in space and then defines the topographic control on the location of shallow landsliding.

We define four stability classes that describe the elements within a catchment for a particular simulation: unconditionally unstable, unstable, stable, and unconditionally stable. Unconditionally unstable elements are those predicted to be unstable even when dry. Unstable elements are those predicted to fail according to (4). Stable elements have insufficient catchment area (and hence wetness) to fail. Unconditionally stable elements are those predicted to be stable even when saturated.

These stability categories can be defined on a plot of either wetness, or drainage area per unit contour length versus slope (Figure 2). As mentioned above, wetness cannot exceed 1.0 in this model (equation (3a)). Hence the range of values is from 0.0 to 1.0. Equation (3b) shows that the threshold of instability is defined by a linear relationship between wetness and ground slope ($\tan \theta$). Ground is unconditionally stable when $\tan \theta \leq \tan \phi [1 - (\rho_w/\rho_s)]$. Unconditionally unstable ground occurs where $\tan \theta > \tan \phi$. Consequently, these slopes should tend to consist of exposed bedrock. The stability of each topographic element may be shown by plotting its position on Figure 2a relative to these boundaries.

Different ratios of soil transmissivity to the rainfall rate (T/q) alter the wetness value for each element. For a given soil transmissivity, a series of simulations with a range of steady state rainfall intensities illustrates the effect of storms

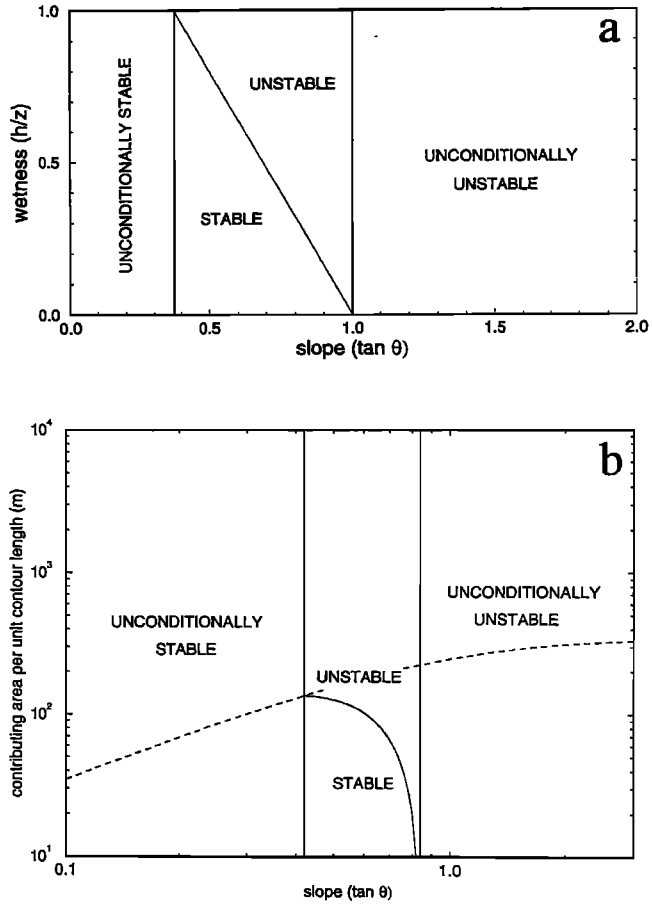

Figure 2. Definition of stability fields on plots of (a) wetness versus slope ($\tan \theta$) and (b) contributing area per unit contour length versus slope ($\tan \theta$). Dashed line represents threshold of ground saturation.

of different intensities. For potentially unstable elements, wetness will increase with increasing q until the stability threshold is crossed. Once this threshold is crossed, an element will remain unstable at greater rainfall rates. Thus we may determine the minimum steady state rainfall predicted to cause instability, here called critical rainfall (q_{cr}), in each element by rearranging (4):

$$q_{cr} = [T \sin \theta (\rho_s/\rho_w)/(a/b)][1 - (\tan \theta/\tan \phi)]. \quad (5)$$

Topographic elements with equal critical rainfall are interpreted to have equal topographic control on shallow landslide initiation. Thus the spatial distribution of critical rainfall values expresses the potential for shallow landslide initiation.

Study Areas

Study areas (Figure 3) were selected on the basis of the availability of high-resolution digital elevation data in debris-flow-prone terrain. Previous field work in these areas allows estimation of both the soil and hydrologic parameters required by the model, albeit with considerable uncertainty about the spatial average. Although the spatial variability of each of these parameters could be included in model simulations, they are treated as spatially uniform because more detailed information on soil properties is unavailable.

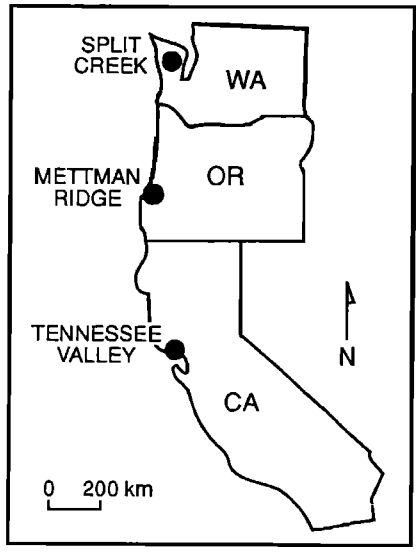

Figure 3. Location map for Tennessee Valley, Mettman Ridge, and Split Creek study areas.

Marin County, California

The Marin County catchment occupies 1.2 km^2 in the Tennessee Valley area of the Marin Headlands just north of San Francisco, California. The area has broad convex hilltops and alluvium-filled major valleys. The catchment is underlain by stacked thrust sheets composed of Cretaceous greenstone, greywacke, and chert of the Franciscan Complex [*Warhaftig*, 1984]. Vegetation is composed of coastal scrub and grasslands communities. The area has a Mediterranean climate with a mean annual rainfall of about 760 mm. Burrowing activity is the dominant sediment transport processes on convex hillslopes and ridgetops [*Lehre*, 1982; *Black and Montgomery*, 1991]; landsliding is an important sediment transport process on steeper side slopes and in topographic hollows, and overland flow and seepage erosion dominate on lower-gradient slopes [*Montgomery and Dietrich*, 1988, 1989; *Dietrich et al.*, 1993]. Further description of geomorphic processes in this catchment is presented elsewhere [*Montgomery*, 1991].

Aerial photography and field inspection identified 43 scars (Figure 4). Earlier analyses reported 39 scars [*Dietrich et al.*, 1992, 1993], but four more have since been identified. Based on vegetation regeneration in the scars, we interpret that most of the landslides occurred during or since storms in 1974 that caused debris flows in Marin County [*Lehre*, 1982]. The maximum scar size is roughly 10 m wide by 20 m long and 1 m deep, similar to the findings of *Reneau and Dietrich* [1987a] in a nearby area. Most of the shallow landslides involved colluvial soils and some scoured to bedrock. Almost all scars were located in steep portions of the catchment, typically either at channel heads or on side slopes.

Dietrich et al. [1992, 1993] generated high-resolution digital elevation data for this catchment from low-altitude, stereo aerial photographs. They also used the program TOPOG to map topographic attributes associated with threshold process theories and thereby divided the catchment into areas dominated by diffusive sediment transport, overland flow, nonerosive overland flow, and landsliding. We use the same digital elevation data set contoured at a 5-m interval in our analysis of this catchment. Unlike their work, we plot potential instability as a function of T/q. We also use a smaller flow net in TOPOG, which reduces the extent of predicted instability.

Field work in this and neighboring areas provides the basis for estimating values for the soil thickness, conductivity, and bulk density. Soil thickness varies from 0.1 to 0.5 m on topographic noses to depths of up to 4.0 m in topographic hollows [*Wilson and Dietrich*, 1987; *Montgomery*, 1991]. The saturated conductivity of the soil varies from 10^{-3} m/s at soil depths less than 1 m to 10^{-10} m/s for soil depths between 3 and 4 m [*Montgomery*, 1991]. The transmissivity of the soil profile is dominated by near-surface soils due to this dramatic decrease in conductivity with increasing soil depth. Based on these and other data, *Dietrich et al.* [1992] estimate the transmissivity of saturated soil profiles in this catchment to be 17 m^2/d, saturated bulk density to be 2000 kg/m^3, and the friction angle to be about 40°. We assume that these values represent the natural heterogeneity within this catchment.

Mettman Ridge, Oregon

The Oregon study site consists of a 0.3 km^2 drainage basin along Mettman Ridge in the Coast Range just north of Coos Bay, Oregon. As is typical in the Oregon Coast Range, the area is highly dissected and characterized by narrow ridgetops and steep slopes. Bedrock consists of gently dipping Eocene sandstone [*Beaulieu and Hughes*, 1975]. The study area was recently clear cut and replanted with Douglas fir, has a maritime climate, and receives approximately 1500 mm of precipitation annually. Shallow debris flows periodically deliver the colluvial soils to the downslope channel system. Further descriptions of the geomorphic processes active in this and adjacent catchments are given elsewhere [*Anderson et al.*, 1990; *Montgomery et al.*, 1990; *Torres et al.*, 1990; *Montgomery*, 1991].

Nineteen shallow landslides occurred in the Mettman Ridge catchment between forest clearance in 1987 and the summer of 1992 (Figure 4b). Six shallow landslides located immediately below a logging road were associated with drainage concentration and/or fill berm failures. The other debris flows occurred within clear cuts and had typical dimensions of 5 m by 10 m with a depth of about 1.5 m. Six of these debris flows occurred in hollows at the heads of first-order channels. Three of the remaining seven occurred in subtle hollows not depicted on the topographic map; four occurred on steep slopes next to channels. Much of the coarser debris was deposited within the study catchment, with most coming to rest at tributary junctions. Storms observed to cause shallow landslides in this catchment had annual or biennial 24-hour rainfall intensities of 50–75 mm/d. Contemporary sediment transport rates from landsliding greatly exceed long-term rates calculated from the basal age of colluvial deposits in topographic hollows, indicating a significant postlogging increase in sediment transport by debris flows [*Montgomery*, 1991].

Digital elevation data were generated from a 1:4800 scale topographic map of the catchment constructed from low-altitude aerial photographs obtained prior to clear cutting. During field work, several significant discrepancies were noted between the actual landform and that portrayed on the base map; nonetheless, it is the best available map of the catchment. The vectorized data were gridded and then

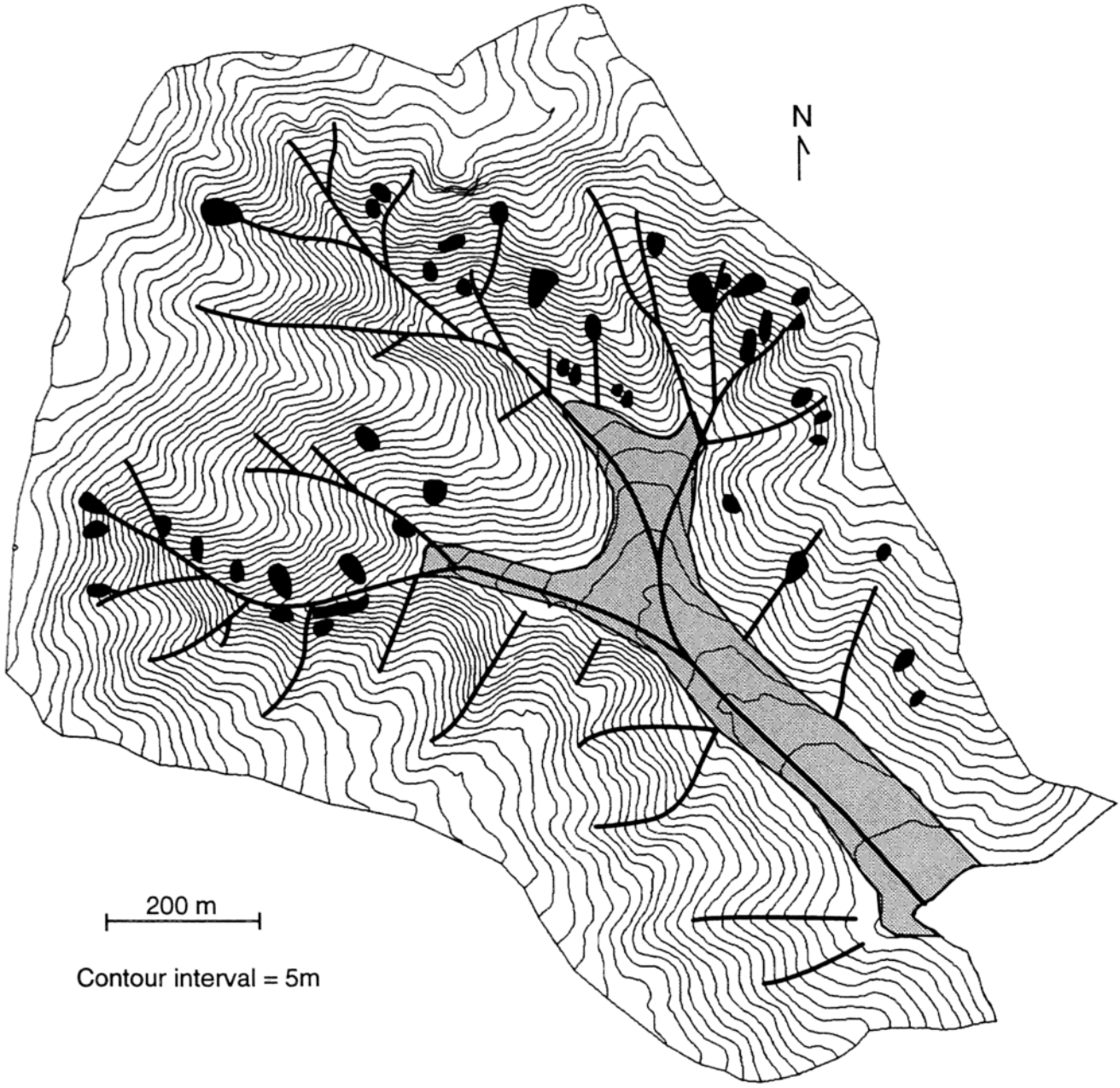

Figure 4a. Topographic map of the Tennessee Valley study catchment showing distribution of landslides, channels, and debris flow deposits. Landslide symbols are shown larger than scars are in the field because of uncertainty associated with field mapping. In Tennessee Valley, deposits in major valleys are composed of interstratified alluvial and debris flow deposits.

contoured at the interval of the original base map using the program TOPOG, resulting in digital contours that are essentially identical to the original contours. Analysis was conducted using a map with a 5-m contour interval constructed from this data set.

Field work in these catchments and similar areas of the Oregon Coast Range provides constraints on the soil bulk density and transmissivity. The colluvial soil in the study area is a silty sand that ranges in thickness from roughly 0.1 to 0.5 m on topographic noses to greater than 2 m in topographic hollows [*Montgomery*, 1991]. Bedrock crops out in many areas where the slope exceeds 45°. Saturated hydraulic conductivity of the colluvial soil declines from about 10^{-3} m/s at the ground surface to about 10^{-4} m/s at a depth of 2 m [*Montgomery*, 1991]. Based on these data, we estimate that an appropriate transmissivity for use in this catchment is 65 m^2/d. Saturated soil bulk density is about 1600 kg/m^3 (R. Torres et al., manuscript in preparation, 1993). Reported values of the angle of internal friction for soils developed on sandstones in the Oregon Coast Range vary from about 35° to 44° [*Yee and Harr*, 1977; *Schroeder and Alto*, 1983; *Burroughs et al.*, 1985], with substantially lower values for saturated soils due to disaggregation upon wetting [*Yee and Harr*, 1977]. Root strength of both coniferous and understory vegetation provides significant apparent cohesion to the soil. Inclusion of the apparent cohesion

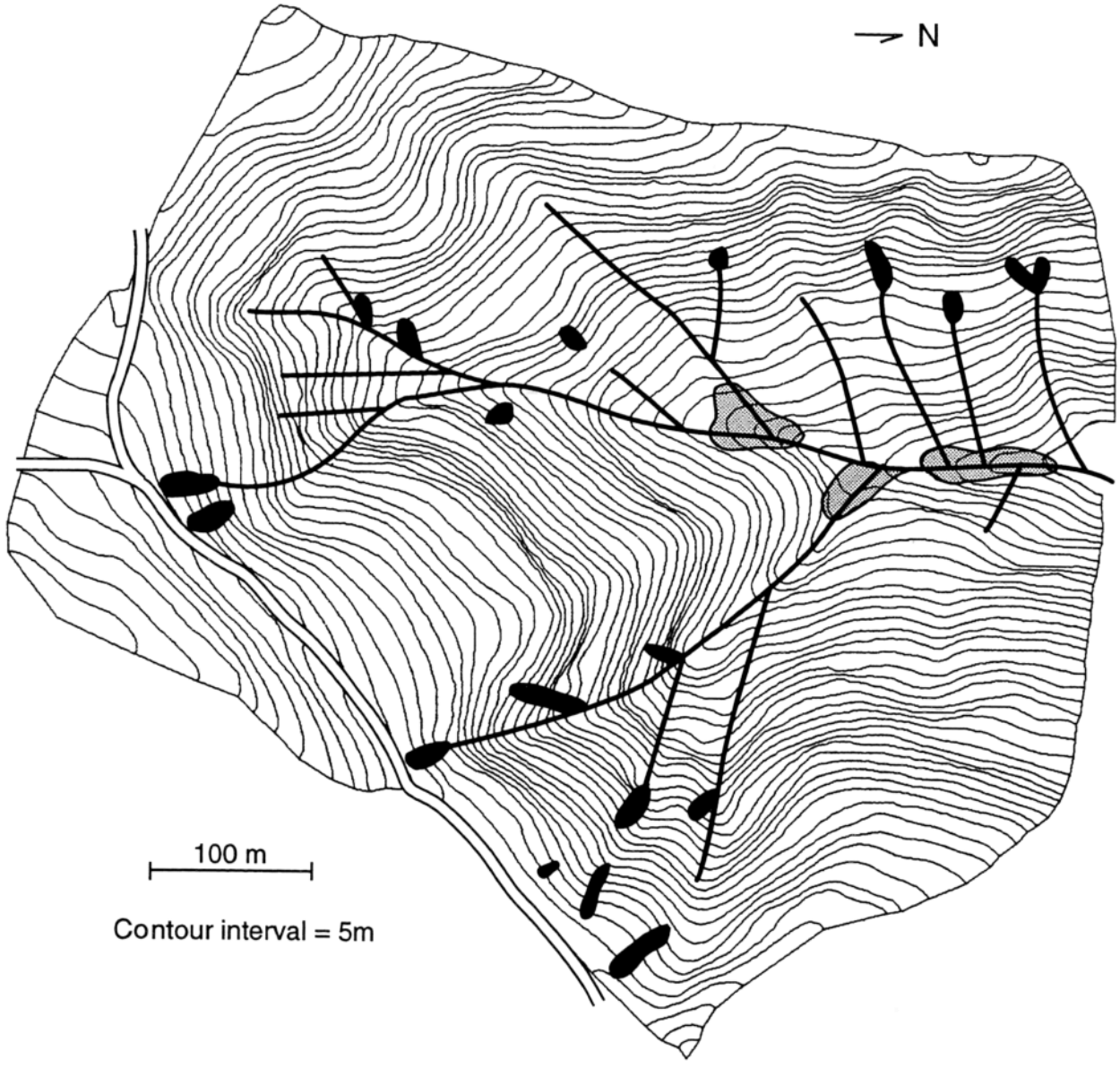

Figure 4b. Same as Figure 4a except for Mettman Ridge study catchment.

due to root strength requires local data on soil depth. Although we recognize that the strength effect of cohesion cannot be fully accounted for by increasing the friction angle, we have no other option in this simple model. Here we adopted a friction angle of 45°, increasing the soil strength as much as 1.4 times the actual frictional strength.

Split Creek, Washington

The Olympic Peninsula study area encompasses the west fork of Split Creek, a 0.6 km^2 basin on the north flank of Huelsdonk Ridge on the South Fork of the Hoh River. The area is characterized by steep, unglaciated tributaries that drain into wide, glaciated valleys filled with outwash and Holocene alluvial sediments. Huelsdonk Ridge is underlain by steeply dipping, folded and faulted Oligocene to upper Eocene sandstone [*Tabor and Cady*, 1978]. The area receives from 4000 to 5000 mm/yr of rainfall annually and was covered by a primarily western red cedar forest prior to clear cutting of the basin in the 1980s.

Colluvial soils developed on sandstones in this area are silty sands with a saturated bulk density of about 1800 kg/m^3 [*Schroeder and Alto*, 1983]. Soil thickness averages about 1 m [*Schlichte*, 1991], although soils are shallower on topographic noses and thicker in hollows. *Schroeder and Alto* [1983] reported a friction angle of 36° for a recompacted sample from colluvial soils developed on sandstone in this part of the Olympic Peninsula. Again, we adopt a friction angle of 45° to compensate for the effective cohesion provided by root strength of the second growth forest and understory. No data are available on the hydraulic conductivity of the colluvial soils in this area, but based on experience in similar soils in the Oregon Coast Range, we estimate a transmissivity of about 65 m^2/d for this catchment.

Digital elevation data were generated from color aerial photographs using a stereo-digitizer. The ground surface was sampled at an average spacing of 5 m and contoured at a 5-m interval (Figure 4c). Landslides visible on color aerial pho-

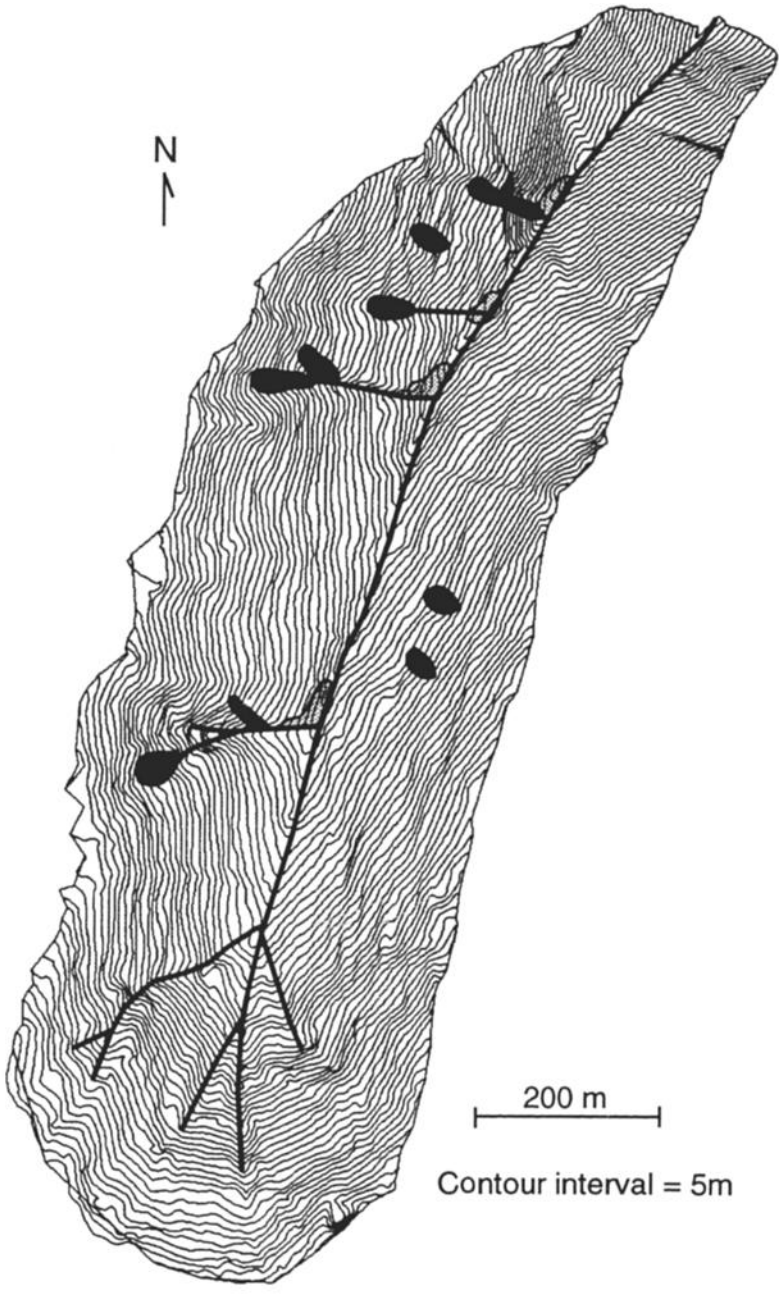

Figure 4c. Same as Figure 4a except for Split Creek study catchment.

tographs flown in 1990 were mapped onto this base map. Landslide frequency in surrounding areas increased by 600–700% in the decade following forest clearance [*Schlichte*, 1991]. In the west fork of Split Creek, nine shallow debris flows were mapped. Five of the failures occurred at the head of first-order channels, one occurred at the base of a hillslope along a channel, and three occurred on steep side slopes.

Simulations

The model may be run in several different formats. Element stability may be simulated for a steady state rainfall intensity, or alternatively, the critical rainfall necessary to cause instability may be determined for each topographic element. The former approach illustrates model performance, but the latter approach is most useful for hazard assessment.

A series of simulations for the Mettman Ridge catchment illustrates the effect of increasing q on predicted instability. At a rainfall intensity of 20 mm/d, most topographic elements lie within the stable field on a plot of wetness versus slope (Figure 5a). With increasing rainfall (Figures 5b and 5c), the wetness value for each topographic element increases, and progressively more of the catchment plots as either unstable or not steep enough to fail. Every element where $[1 - (\rho_w/\rho_s)] \tan \phi < \tan \theta < \tan \phi$ is potentially unstable with a sufficiently high rainfall rate.

The map distribution of predicted instability provides a

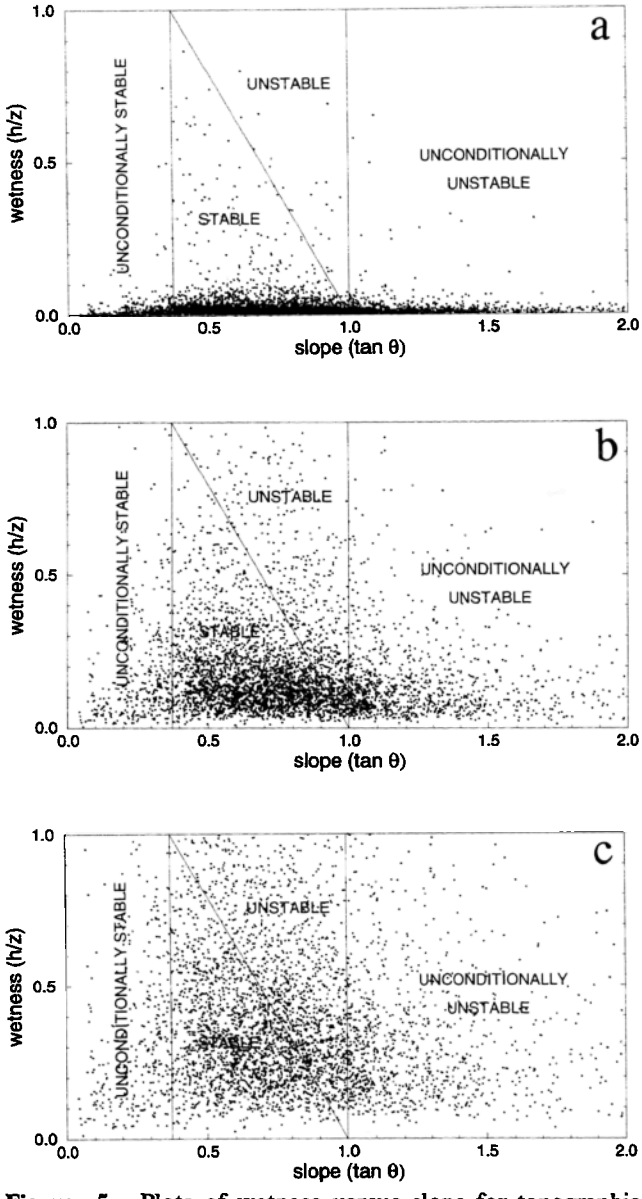

Figure 5. Plots of wetness versus slope for topographic elements in Mettman Ridge study catchment (T = 65 m^2/d, tan ϕ = 45°, and ρ_s = 1600 kg/m^3) for (a) q = 20 mm/d; (b) q = 100 mm/d; and (c) q = 200 mm/d.

spatial context within which to interpret these simulations, as well as constraints on reasonable values of q. At 20 mm/d rainfall, most of the catchment is stable (Plate 1a), except for areas of unconditional instability that coincide with the observed pattern of local bedrock outcrops. These zones are areas where slopes are too steep to allow the accumulation of significant soil. They are unlikely to generate shallow landslides. Increasing the rainfall rate to 100 mm/d (Plate 1b), zones of predicted instability spread to steep, low-order channels, topographic hollows, and base of steep side slopes. Further increasing the simulated rainfall to 200 mm/d (Plate 1c) expands the zones of predicted instability away from channels, toward drainage divides, and into topographically divergent hillslopes where debris flow initiation is rare.

Relative Failure Potential

The map pattern of the critical rainfall predicted by (5) provides a prediction of relative potential for shallow landslide initiation. Elements with lower q_{cr} are interpreted as more susceptible to shallow landsliding. Conversely, elements with higher q_{cr} are interpreted as more stable, as a less frequent rainfall event would be required to cause instability. While the absolute value of q_{cr} for any topographic element depends on the values of ρ_s, tan ϕ, and T, the topographic parameters (a/b, tan θ) control the relative patterns of predicted q_{cr} values if the soil properties are spatially constant.

The three study catchments differ in the extent of the zone of potential instability (Plate 2). The Marin County study site has predominantly gentle slopes compared to the assumed friction angle, and only a third of the catchment area is potentially subject to shallow landsliding, even in response to extreme hydrologic events. In contrast, the Mettman Ridge and Split Creek catchments are much steeper and most of these catchments are potentially unstable.

Comparison of observed landslide locations with model predictions provides a test of model performance (Plate 2). Although it is difficult to precisely compare field observations and model predictions because the uncertainty associated with field mapping is of the order of the size of the topographic elements used in these simulations, we mapped observed landslides onto a map of predicted critical rainfall (Plate 2). Landslide scars are mapped larger than they are in the field because of this uncertainty, and most occupy several topographic elements. Thus the lowest q_{cr} value for the elements overlain by a mapped landslide was considered to reflect the value for the landslide.

A simple test of model performance is to compare the proportion of landslides with different critical rainfall values to the percent of the catchment area with similar values (Table 1). Better model performance would be reflected in a disproportionate occurrence of landslides in sites predicted to have a lower critical rainfall. In each of the study areas, proportionally more landslide scars occupy areas predicted to be least stable (q_{cr} < 50 mm/d).

Two thirds of the Tennessee Valley catchment is not steep enough to fail according to the criterion of (4) (Table 1). Only the steeper slopes along valley margins and at the head of hollows are modeled as susceptible to shallow landsliding. These areas define the general areas in which landslide scars were observed. Furthermore, many low-order channels in these steeper parts of the catchment occupy elements predicted to be least stable, and a number of channel heads occur in elements in the least stable category. Progressively fewer landslides are located in areas with greater critical rainfall values (Table 2).

Most of the Mettman Ridge catchment is predicted to be unstable at some rainfall rate (Table 1). The pattern of predicted instability, however, changes systematically with increasing rainfall. Steep areas predicted to be unconditionally unstable generally correspond to areas with bedrock exposed at the ground surface (Plate 2b). These areas represent sites of chronic instability where significant material does not accumulate. As rainfall increases to 100 mm/d, zones of predicted instability extend to low-order channels and hollows and onto the base of some steeper hillsides. Most of the low-order channels in this area lack significant

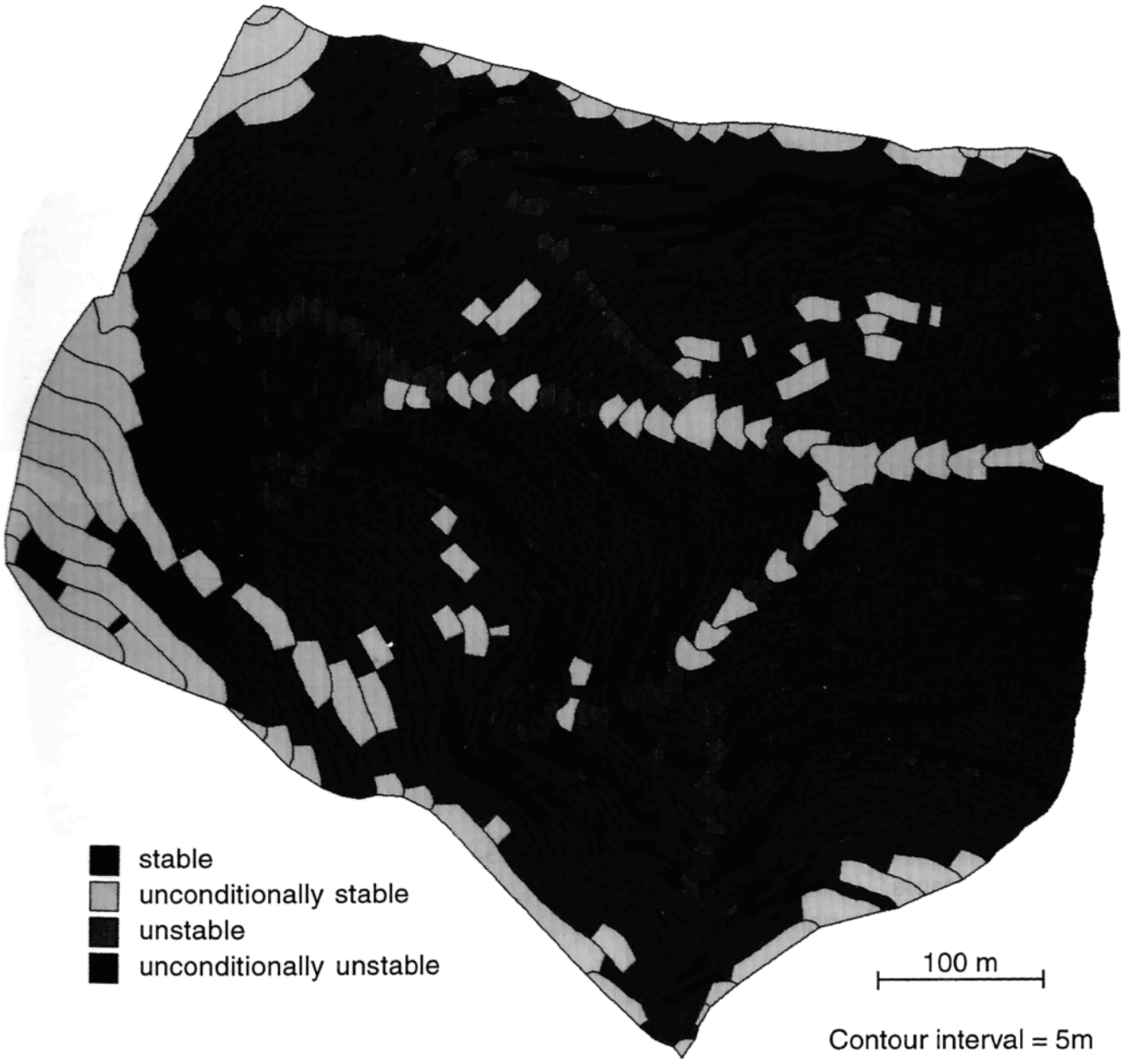

Plate 1a. Map of predicted stability for the Mettman Ridge study catchment (tan $\phi = 45°$, $T = 65$ m^2/d, and $\rho_s = 1600$ km/m^3) for $q = 20$ mm/d.

colluvial valley fill, and most shallow landslide scars occur in hollows and low-order channels (Figure 4b). Field inspection indicates that each of the three scars mapped as occurring on topographic noses occurs in a subtle hollow not reflected on the topographic map. Hence our model cannot detect their instability. At rainfall rates between 100 and 200 mm/d, areas of predicted instability expand farther into hillslopes and up to the heads of valleys until they virtually enclose the valley network. Topographically divergent ridgelines and hillslopes between valleys are unstable only at steady state rainfall in excess of 200 mm/d. Roughly half of the observed landslides occurred in areas predicted to be least stable (Table 2).

Almost the entire Split Creek catchment also is predicted to be unstable at some rainfall intensity (Table 1). Again, steep, low-order channels and the lower end of topographic hollows are predicted to be most susceptible to failure (Plate 2c). At greater rainfall intensities, zones of predicted instability expand farther up hollows and onto the base of surrounding slopes, eventually extending into topographically divergent hillslopes. All of the observed landslide scars occur in topographic hollows or on steep side slopes in areas predicted to be least stable (Table 2).

In each of these catchments, landslides occurred with disproportionate frequency in areas predicted to be least stable (Table 2). This comparison of predicted patterns of relative stability and observed patterns of shallow landsliding indicates that q_{cr} provides a reasonable proxy for failure potential. Furthermore, there are similarities in the pattern of q_{cr} between the catchments. In general, steep convergent areas, such as low-order channels and hollows, are most susceptible to failure. Steep side slopes and smaller or lower-gradient hollows are next, and divergent hillslopes are

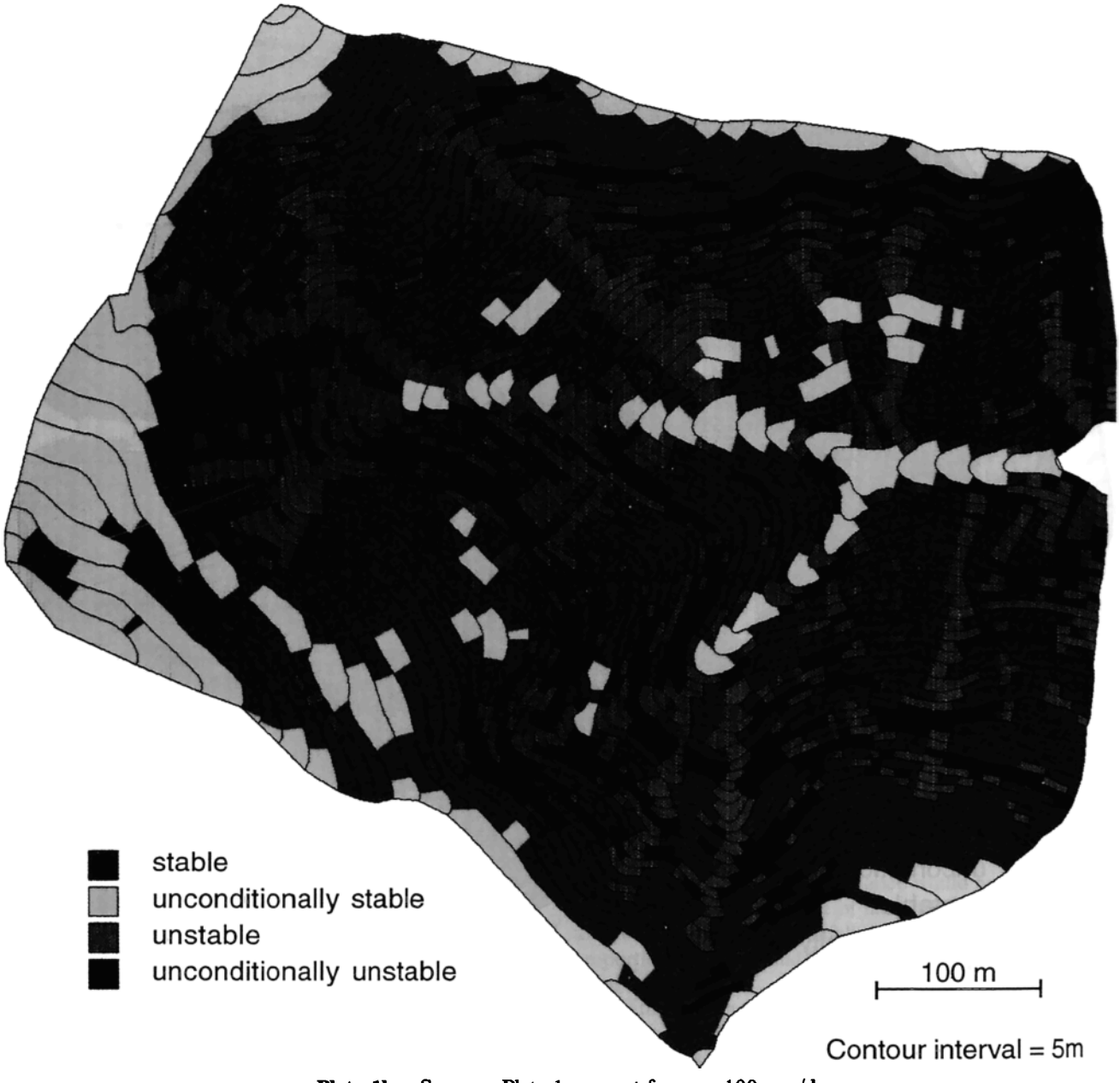

Plate 1b. Same as Plate 1a except for q = 100 mm/d.

least susceptible to failure. This pattern corresponds well with results of other field surveys, which indicate that the majority of debris flows originate in topographic hollows but that a significant percentage also originate on steep side slopes and channel margins [e.g., *Okimura and Ichikawa*, 1985; *Reneau and Dietrich*, 1987a; *Ellen et al.*, 1988]. Shallow landsliding from divergent ridgetops and topographic noses is rare.

In each of the study areas, many more areas are predicted to be unstable than are observed to have failed in the field. Five years of observations in the Mettman Ridge catchment indicate that small, shallow debris flow scars rapidly heal and are difficult to detect after as few as 3 years. Our field and aerial photo mapping only captures the most recent failures, and many of the areas predicted to be unstable may have failed at some time in the past. Although it also is possible that the model overrepresents areas potentially subject to shallow landsliding, slope morphology in zones of predicted failure suggests that they represent areas in which landsliding dominates sediment transport and slope evolution. The majority of slopes predicted to be unstable are neither convex nor concave but rather are planar in profile, a shape consistent with long-term erosion by landsliding. Consequently, we judge that zones of predicted instability generally represent areas in which landsliding is a major sediment transport process over long timescales.

Constraints on the Hydrologic Parameters (T/q)

Observed areas of soil saturation effectively constrain reasonable values of the hydrologic parameters (T/q) and

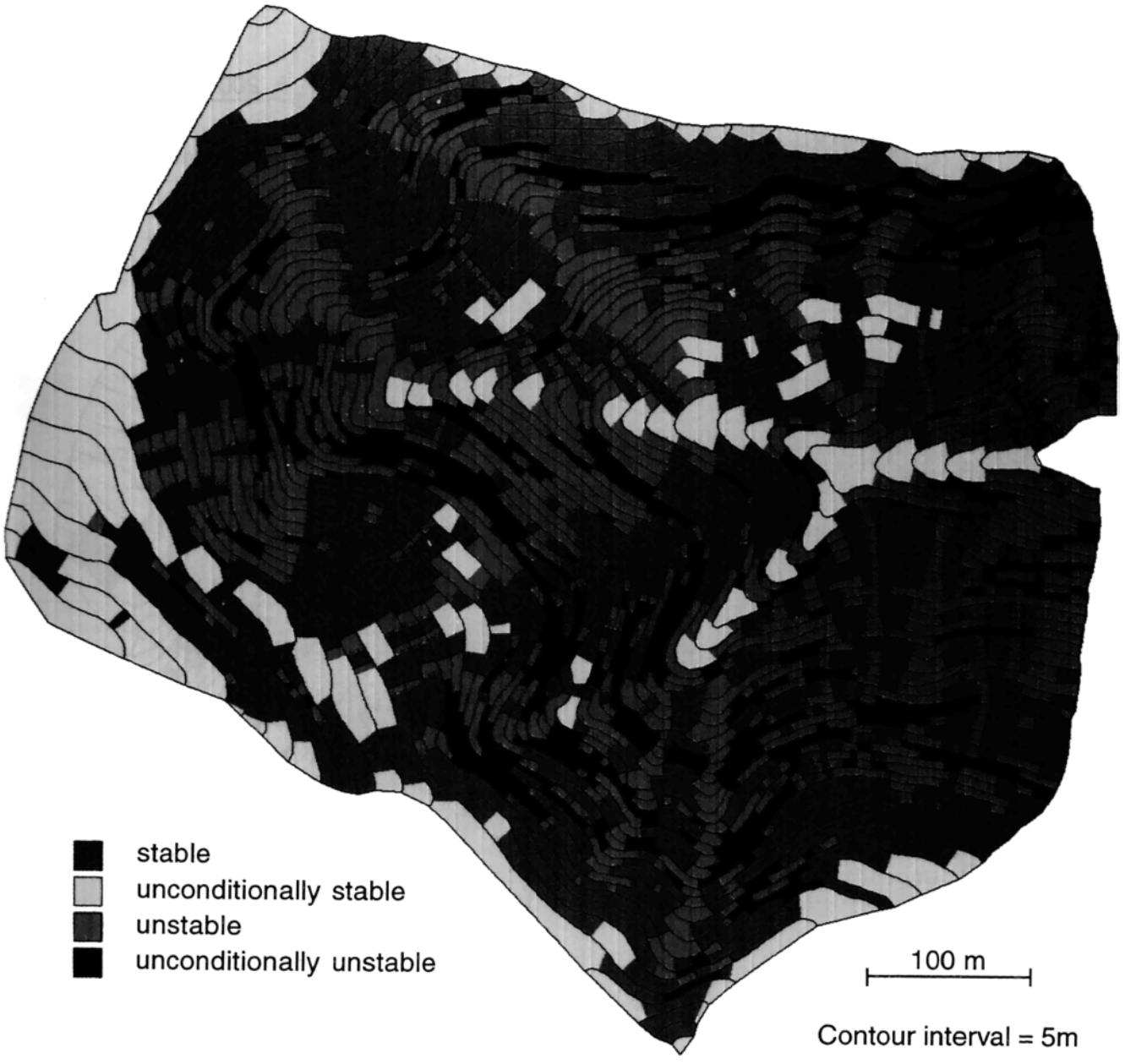

Plate 1c. Same as Plate 1a except for q = 200 mm/d.

thus provide an upper limit to the critical rainfall. In each of the study catchments, overland flow only rarely, if ever, occurs on topographically divergent hillslopes. Consequently, a reasonable limit to the steady state rainfall for use in slope stability simulations is provided by the rainfall in excess of which saturated zones expand into divergent portions of the landscape.

The steady state rainfall necessary to saturate a topographic element q_s is given by

$$q_s = (bT/a) \sin \theta. \quad (6)$$

This criterion also may be expressed interms of the ratio T/q

$$T/q = a/b \sin \theta. \quad (7)$$

For the Tennessee Valley catchment, the rainfall rate above which saturation spreads into divergent elements is about 50 mm/d (T/q = 350 m), whereas for the Mettman Ridge and Split Creek catchments it is about 200 mm/d (T/q = 325 m) (Figure 6). These values of the critical rainfall may be used as limits for the steady state rainfall used to predict zones of potential instability. The majority of observed landslides in the study areas are within zones of predicted instability so determined.

In the Tennessee Valley catchment, 33 of the 43 debris flow scars (78%) identified in the study area include elements predicted to be unstable using the hydrologic constraint for saturation of divergent topography ($q \leq 50$ mm/d). For the Mettman Ridge catchment, 16 out of 19 debris flow scars

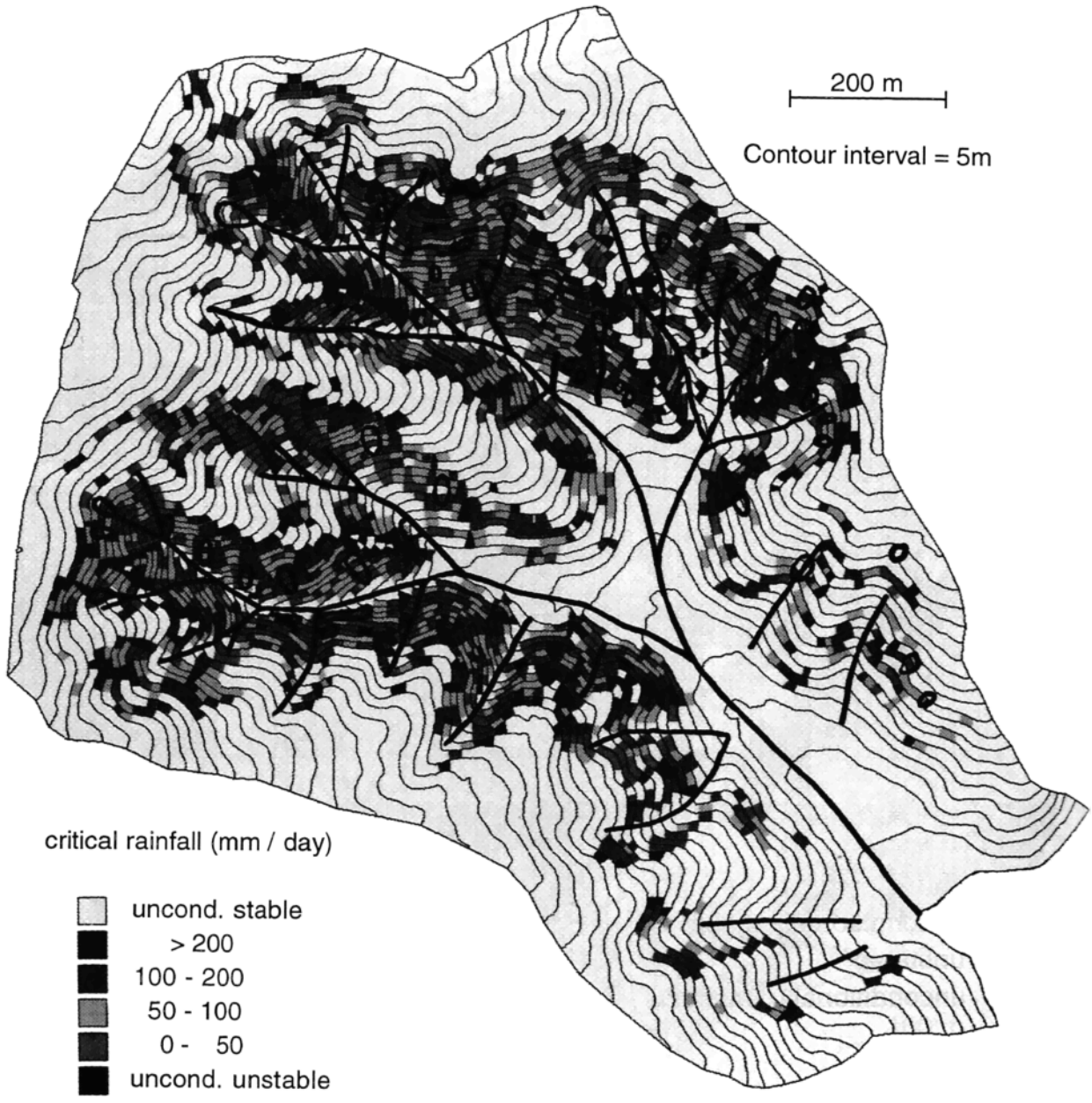

Plate 2a. Map showing steady state rainfall intensity [mm/day] necessary for slope instability in each topographic element for Tennessee Valley (tan $\phi = 40°$, $T = 17$ m^2/d, $\rho_s = 2000$ kg/m^3).

(84%) include locations predicted to be unstable ($q \leq 200$ mm/d). Two of the other three landslide scars were associated with road drainage concentration. The final unexplained debris flow scar is located at the downslope end of a hollow not portrayed on the topographic basemap used to create the digital elevation data. In the Split Creek catchment, all of the observed scars are in locations that include elements predicted to be least stable (Table 2). These examples illustrate that observed debris flow scars generally occur in locations predicted by the model to be susceptible to debris flow initiation, indicating that this approach provides a simple assessment of relative debris flow initiation hazard.

It is curious, however, that the limiting value of the hydrologic parameter T/q is similar for each of the study areas. While we are not certain of the significance of this observation, it reflects the similar size of the convex, diffusion-dominated portions of the hillslopes in these areas. Acquisition of high-resolution digital elevation data from additional areas will allow further exploration of this observation.

Debris Flow Routing

Mobilization of shallow landslides into debris flows reflects soil properties [e.g., *Ellen and Fleming*, 1987] that cannot be predicted directly from digital elevation models. However, such models can be used to predict potential run out paths in debris-flow-prone areas. There are many approaches to delineating down slope areas potentially impacted by debris flows [e.g., *Ikeya*, 1981; *Takahashi*, 1981; *Benda and Cundy*, 1990; *Ellen et al.*, 1993]. Here we apply a simple algorithm for delineating areas subject to different styles of debris flow impact.

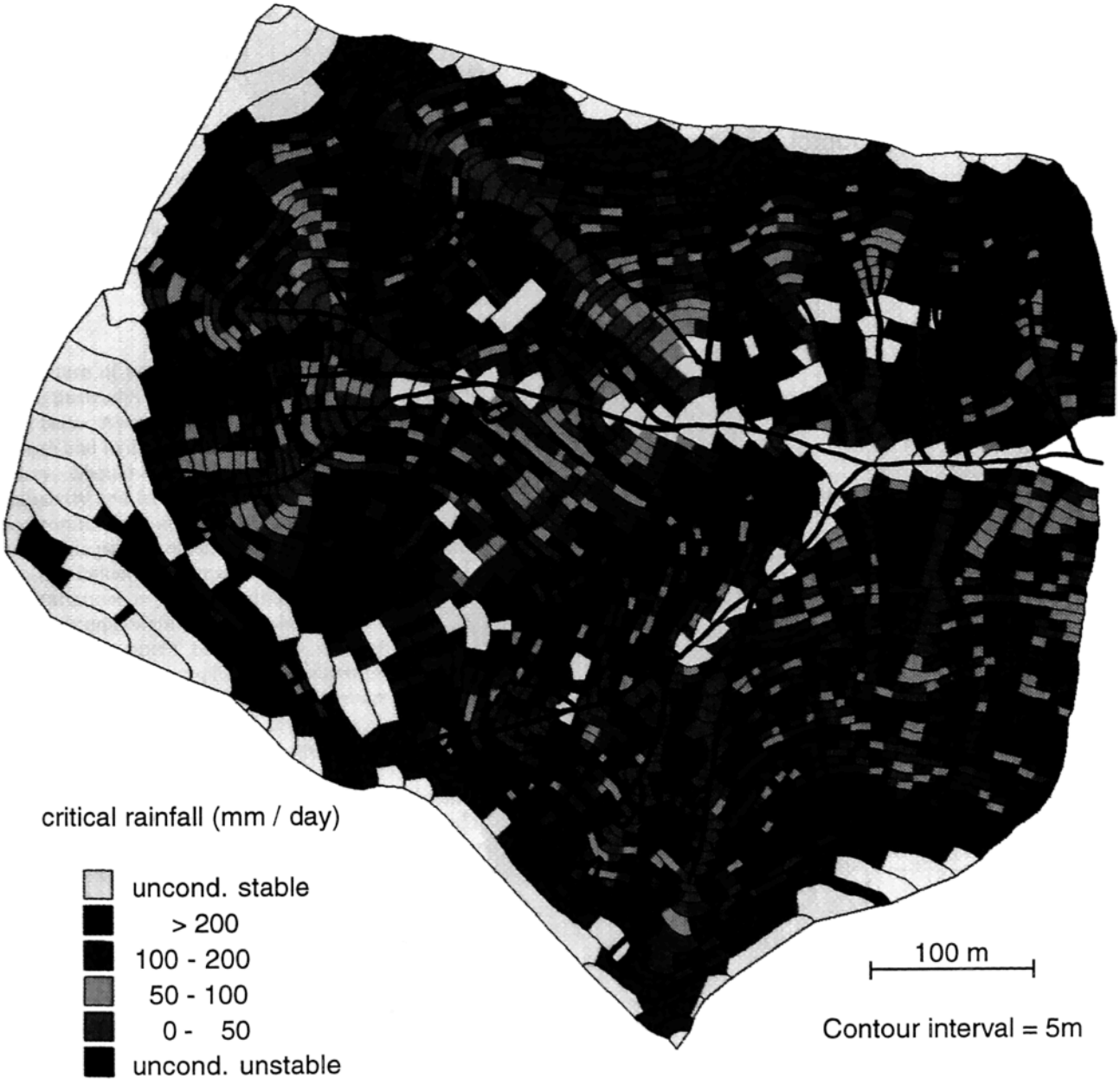

Plate 2b. Same as Plate 2a except for Mettman Ridge (tan $\phi = 45°$, $T = 65$ m^2/d, $\rho_s = 1600$ kg/m^3).

Relative debris flow hazards differ for initiation, transport, and deposition areas. The flow tube architecture of TOPOG facilitates determination of debris flow paths and allows gross characterization of debris flow behavior along these paths. For a given simulation, elements that are unstable according to (4) define potential sites of debris flow initiation. Potential debris flow paths are traced down flow tubes until a depositional criterion is exceeded. In reality, a debris flow will be deposited when it thins or flows onto a slope gentle enough that the forces driving continued motion are less than the yield strength of the flowing material. This often occurs on slopes between roughly 3° and 6° [e.g., *Campbell*, 1975; *Ikeya*, 1981; *Takehashi et al.*, 1981; *Benda and Cundy*, 1990], but incorporation of large woody debris into the snout of a moving debris flow, or momentum extraction associated with high-angle tributary junctions, may force deposition on steeper slopes. Here we define a zone of likely debris flow deposition as the first set of consecutive topographic elements within a prescribed slope range down a flow tube from an element predicted to be unstable. Transport zones are delineated as the topographic elements along the flow tube between initiation and deposition points.

For the Tennessee Valley study area, this algorithm predicts that the steep channels in the basin headwaters transport debris flows, while the lower-gradient channels in the major valleys are within depositional zones (Plate 3). These patterns correlate well with the observed distribution of bedrock channels and Holocene valley fills composed of interstratified debris flow and alluvial deposits (Figure 4a). Channels in the Mettman Ridge and Split Creek study areas are too steep to allow deposition according to the criteria given above. However, a number of debris flow deposits are

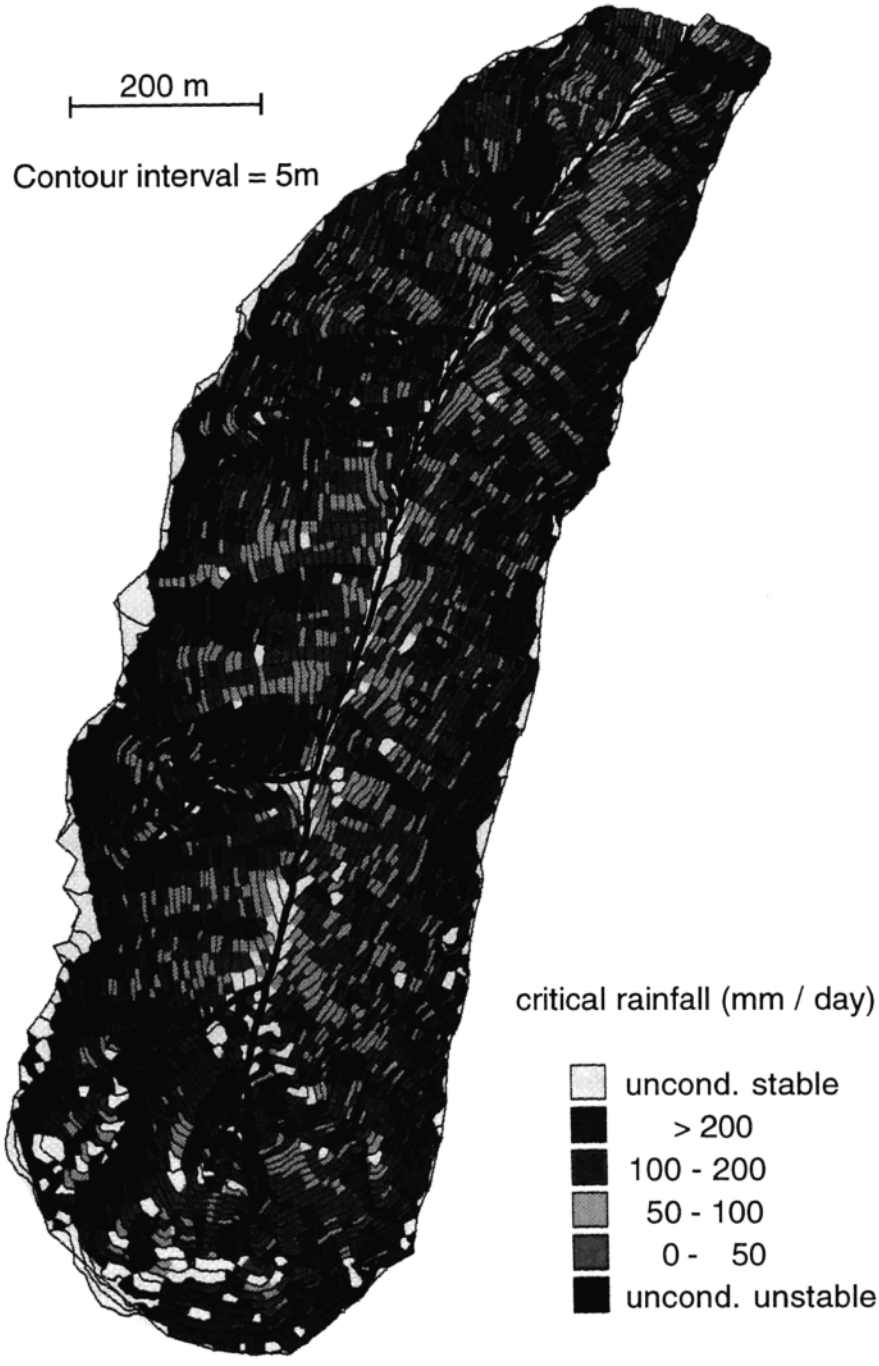

Plate 2c. Same as Plate 2a except for Split Creek (tan $\phi = 45°$, $T = 65$ m^2/d, $\rho_s = 1800$ kg/m^3).

located at channel confluences or behind log jams. Such deposits are subject to scour by subsequent debris flows, and we have found what appear to be multiple debris flow deposits in low-gradient reaches at the mouth of the creeks draining both the Mettman Ridge and Split Creek study areas.

This approach provides a preliminary method for predicting potential debris flow runout paths. More complex algorithms are desirable to represent potential zones of deposition at tributary confluences and to account for the effect of large woody debris. The approach presented here provides a simple method for characterizing areas potentially subject to different styles of debris flow impacts.

Discussion

This model is intended to be simple; it delineates those areas most prone to shallow landsliding due to surface topographic effects on hydrologic response. This is most appropriate for modeling topographically controlled shallow landsliding common in steep highly dissected, soil-mantled topography. Although the assumptions incorporated in the model, especially the steady state hydrologic model, preclude its use as a tool to predict the frequency of landslide initiation, the model does assess relative stability as expressed by the critical steady state rainfall. Our steady state hydrologic model requires the assumption that the predicted

Table 1. Percent of Catchment Area in Each Critical Rainfall Range

Critical Rainfall, mm/d	TV	MR	SC
Unconditionally unstable	1	13	9
0–50	8	10	8
50–100	9	7	10
100–200	10	13	19
>200	5	42	44
Unconditionally stable	67	16	10

TV, Tennessee Valley; MR, Mettman Ridge; SC, Split Creek.

spatial pattern of pore pressures mimics that which occurs during an unsteady, landslide-producing rainfall event. This may not be so. Assumptions regarding the spatial uniformity of strength and hydrologic properties are convenient but not necessary. Should such data as the spatial variation in transmissivity and frictional strength be available, they can be incorporated into model simulations.

The specific pattern of landsliding observed in a catchment reflects the influence of many factors not included in the model. Variations in soil strength and transmissivity impart a stochastic component to shallow landslide initiation. While these properties could be assigned to each topographic element by randomly sampling from a distribution of potential values, we feel that a Monte Carlo approach to predicting the spatial distribution of soil properties only serves to obscure the topographic influence on slope instability and give a false sense of relative stability. Soil thickness may exhibit both stochastic local variability and systematic differences associated with topographic position. Unfortunately, detailed information on soil thickness is only rarely available. The seepage force necessary to destabilize a slope depends on the flow orientation [*Iverson and Major*, 1986], and field studies in both the Tennessee Valley and Mettman Ridge study areas indicate that the hydrologic characteristics of the near-surface bedrock strongly influence the piezometric response in the overlying colluvium [*Wilson and Dietrich*, 1987; *Montgomery et al.*, 1990; *Montgomery*, 1991]. Although this influences slope stability, it is difficult to include in a model without detailed knowledge of bedrock fracture patterns. The effective cohesion provided by root strength which has not been explicitly included also is spatially

Table 2. Percent of Landslides in Each Critical Rainfall Range

Critical Rainfall, mm/d	TV	MR	SC
Unconditionally unstable	0	0	0
0–50	81	47	100
50–100	15	26	0
100–200	2	11*	0
>200	2	16*	0
Unconditionally stable	2	0	0

TV, Tennessee Valley; RM, Mettman Ridge; SC, Split Creek.

*These landslides either were associated with road drainage concentration or were in subtle topographic hollows not resolved in the digital topography.

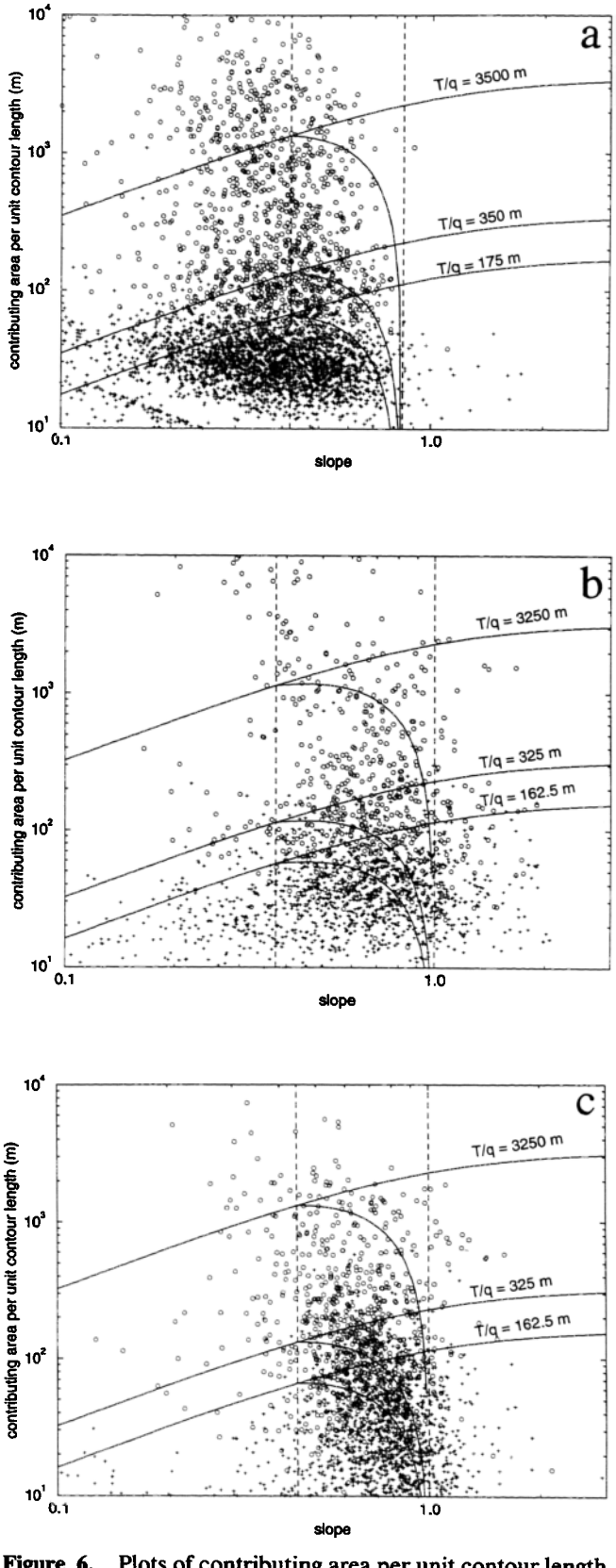

Figure 6. Plots of contributing area per unit contour length versus slope (tan θ) for convergent (circles) and divergent (crosses) topographic elements in the (a) Tennessee Valley, (b) Mettman Ridge, and (c) Split Creek study catchments showing the effect of varying T/q on the topographic thresholds for soil saturation and slope stability (solid lines). Dashed lines indicate limits of the slope stability model.

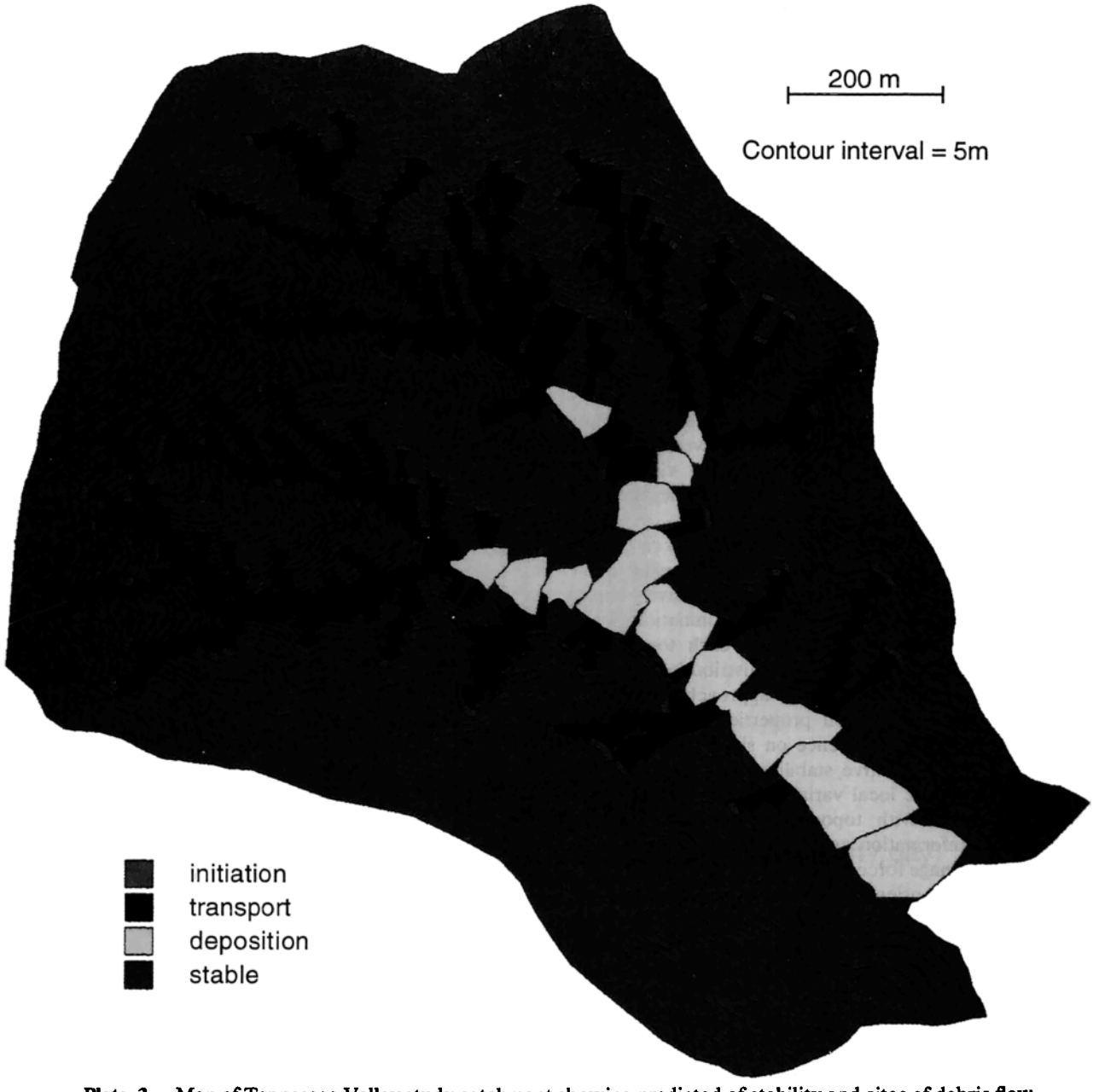

Plate 3. Map of Tennessee Valley study catchment showing predicted of stability and sites of debris flow initiation, transport, and deposition (q = 50 mm/d; tan ϕ = 40°, T = 17 m^2/d, and ρ_s = 2000 kg/m^3).

variable and difficult to estimate. Where detailed local information about the landscape and its soils are unavailable and, in practice, too costly to quantify, we propose that this simple model of the topographic control on landslide initiation and debris flow run out is useful. In essence, we propose that even though specific sites of landsliding are largely unpredictable, relative slope stability can be roughly delineated.

Several additional qualifications apply to the application of digital terrain models to geomorphic processes. These concern the quality of the data, the relevance of the model to specific field applications, and the methods employed to evaluate, constrain, or calibrate the model. In general, simulations based on digital terrain models are only as accurate as the digital elevation data upon which they are based. Unfortunately, many digital terrain models only generally resemble the landscapes from which they are derived. The accuracy and resolution of the topography are especially important in the steep, finely dissected terrain where debris flows are an important process. Low-resolution data bias modeled slopes toward lower gradients [*Zhang and Montgomery*, 1994] and thus may influence predicted zones of instability. Acquisition of high-quality, high-resolution digital elevation data is important to allow resolution of potential debris flow source areas. Without high-quality topographic data, physically based models may yield inaccurate and misleading results.

Estimation of appropriate values for soil and hydrologic parameters requires the experience of a geomorphologist familiar with landslide and runoff generation processes

within the catchment of interest. Experience or field measurements are needed to estimate spatially averaged values for ρ_s, tan ϕ, and T. Some judgement is required to determine an upper limit to the steady state rainfall used to define zones of potential instability. In the end, process-based models for assessment of debris flow hazards are only as valid as the information used to parameterize them. Nonetheless, we feel it is a step forward to have a process-based model that appears to have wide applications and which is based on only a few parameters with a finite range and a physical meaning such that field data can be collected to estimate their value. Moreover, the present model can be made more realistic by adding estimates of spatial variation of soil depth, strength (including cohesion), and transmissivity and by using a dynamic rather than steady state rainfall. It is an open question whether the introduction of poorly constrained and spatially variable parameters that this will require will substantially improve predictions of relative slope stability.

This model also has implications for long-term landform development in steep, soil-mantled terrain. In particular, our analyses indicate that the topographic control on shallow landsliding initiation may be similar for hollows and the lower portions of steep valley walls. This finding is consistent with the hypothesis that an erosional threshold defined in terms of drainage area and slope controls the limit to landscape dissection and thus valley development [*Montgomery and Dietrich*, 1992].

Conclusions

The model described above provides a method for assessing the relative potential for shallow landslide initiation in steep, soil-mantled terrain underlain by low-permeability material. Field observations and landform provide constraints on hydrologic parameters, and estimates of the soil conductivity, thickness, bulk density, and friction angle may be constrained by field observations or measurements. In essence, the model then quantifies the topographic influence on shallow slope stability. Portions of the landscape predicted to be least stable (low-order channels, hollows, and steep side slopes) correspond to locations where debris flows typically initiate (see review by *Montgomery et al.* [1991]). Temporally variable rainfall may be accommodated in future versions of the model but may not be required for relative hazard assessments. Our analysis indicates that coupled hydrologic, slope stability, and digital terrain models provide a powerful tool for assessment of debris flow hazards.

Locations of observed landslide scars support the interpretation that elements with the lowest q_{cr} needed to cause failure are most unstable. However, a practical consideration in using this model is whether elements requiring very high rainfall to become unstable should still be considered hazardous. We believe this question can only be answered in the context of the problem. Even a site that takes an extreme rainfall to mobilize as a landslide constitutes a significant hazard if it lies upslope of either an inhabited structure, such as a private home, or a critical resource, such an the habitat for threatened and endangered species. While our model appears to be of general use in delineating the relative potential for shallow landsliding, the practical application to land use decisions still needs evaluation and requires judgement or values external to the model framework.

Acknowledgments. This project was supported by grants TFW FY92-010 and TFW FY94-004 through the CMER and SHAMW committees of the Washington State Timber/Fish/Wildlife agreement. Harvey Greenberg and Rob Reiss provided analysis, programming, and graphics support. We thank Emmett O'Loughlin and the Australian Center for Catchment Hydrology for the use of TOPOG, Jim McKean for generating the topographic data for Tennessee Valley, and Dave Somers for generating the topographic data for Split Creek. We also thank three anonymous reviewers for their critique of the manuscript.

References

Anderson, S. P., D. R. Montgomery, R. Torres, W. E. Dietrich, and K. Loague, Hydrologic experiments in a steep unchanneled valley, 3, Runoff chemistry dynamics, *Eos Trans. AGU, 71*, 1342, 1990.

Beaulieu, J. D., and P. N. Hughes, Environmental geology of western Coos and Douglas counties, Oregon, *Bull. Oreg. Dep. Geol. Miner. Ind., 87*, 148 pp., 1975.

Benda, L., and T. W. Cundy, Predicting deposition of debris flows in mountain channels, *Can. Geotech. J., 27*, 409–417, 1990.

Benda, L., and T. Dunne, Sediment routing by debris flow, in Erosion and Sedimentation in the Pacific Rim, edited by R. L. Beschta, T. Blinn, G. E. Grant, F. J. Swanson, and G. G. Ice, *IAHS Publ., 165*, 213–223, 1987.

Black, T. A., and D. R. Montgomery, Sediment transport by burrowing mammals, Marin County, California, *Earth Surf. Processes Landforms, 16*, 163–172, 1991.

Brabb, E. E., and B. L. Harrod (Ed.), *Landslides: Extent and Economic Significance*, 385 pp., A. A. Balkema, Rotterdam, Netherlands, 1989.

Brabb, E. E., E. H. Pampeyan, and M. G. Bonilla, Landslide susceptibility in San Mateo County, California, scale 1:62,500, *U.S. Geol. Surv. Misc. Field Stud. Map, MF-360*, 1972.

Burroughs, E. R., Landslide hazard rating for portions of the Oregon Coast Range, in *Proceedings of the Symposium on Effects of Forest Land Use on Erosion and Slope Stability, Honolulu, Hawaii*, edited by C. L. O'Loughlin and A. J. Pearce, pp. 265–274, Environment and Policy Institute, University of Hawaii, Honolulu, 1984.

Burroughs, E. R., Jr., C. J. Hammond, and G. D. Booth, Relative stability estimation for potential debris avalanche sites using field data, in *Proceedings of the International Symposium on Erosion, Debris Flow and Disaster Prevention*, edited by A. Takei, pp. 335–339, Erosion Control Society, Tokyo, 1985.

Caine, N., The rainfall intensity-duration control of shallow landslides and debris flows, *Geogr. Ann., 62A*, 23–27, 1980.

Campbell, R. H., Soil slips, debris flows and rainstorms in the Santa Monica Mountains and vicinity, southern California, *U.S. Geol. Surv. Prof. Pap., 851*, 51 pp., 1975.

Carrara, A., Multivariate models for landslide hazard evaluation, *Math. Geol., 15*, 403–426, 1983.

Carrara, A., E. Pugliese Carratelli, and L. Merenda, Computer-based data bank and statistical analysis of slope instability phenomena, *Z. Geomorphol., 21*, 187–222, 1977.

Carrara, A., M. Cardinali, R. Detti, F. Guzzetti, V. Pasqui, and P. Reichenback, GIS techniques and statistical models in evaluating landslide hazard, *Earth Surf. Processes Landforms, 16*, 427–445, 1991.

Crozier, M. J., E. E. Vaughn, and J. M. Tippett, Relative instability of colluvium-filled bedrock depressions, *Earth Surf. Processes Landforms, 15*, 329–339, 1990.

DeGraff, J. V., Using isopleth maps of landslide deposits as a tool in timber sale planning, *Bull. Assoc. Eng. Geol., 22*, 445–453, 1985.

DeGraff, J. V., and P. Canuti, Using isopleth mapping to evaluate landslide activity in relation to agricultural practices, *Bull. Int. Assoc. Eng. Geol., 38*, 61–71, 1988.

Dietrich, W. E., and T. Dunne, Sediment budget for a small catchment in mountainous terrain, *Z. Geomorphol. Suppl., 29*, 191–206, 1978.

Dietrich, W. E., C. J. Wilson, and S. L. Reneau, Hollows, colluvium, and landslides in soil-mantled landscapes, in *Hillslope Processes*, edited by A. D. Abrahams, pp. 361–388, Allen and Unwin, Winchester, Mass., 1986.

Dietrich, W. E., C. J. Wilson, D. R. Montgomery, J. McKean, and

R. Bauer, Erosion thresholds and land surface morphology, *Geology*, *20*, 675–679, 1992.

Dietrich, W. E., C. J. Wilson, D. R. Montgomery, and J. McKean, Analysis or erosion thresholds, channel networks, and landscape morphology using a digital terrain model, *J. Geol.*, *101*, 259–278, 1993.

Dunne, T., Stochastic aspects of the relations between climate, hydrology and landform evolution, *Trans. Jpn. Geomorphol. Union*, *12*, 1–24, 1991.

Ellen, S. D., and R. W. Fleming, Mobilization of debris flows from soil slips, San Francisco Bay region, California, in Debris Flows/Avalanches: Process, Recognition and Mitigation, edited by J. E. Costa and G. F. Wieczorek, *Rev. Eng. Geol.*, *7*, 31–40, 1987.

Ellen, S. D., and G. F. Wieczorek (Eds.), Landslides, floods and marine effects of the storm of January 3–5, 1982, in the San Francisco Bay region, California, *U.S. Geol. Surv. Prof. Pap.*, *1434*, 310 pp., 1988.

Ellen, S. D., S. H. Cannon, and S. L. Reneau, Distribution of debris flows in Marin County, in Landslides, Floods and Marine Effects of the Storm of January 3–5, 1982, in the San Francisco Bay Region, California, edited by S. D. Ellen and G. F. Wieczorek, *U.S. Geol. Surv. Prof. Pap.*, *1434*, 113–131, 1988.

Ellen, S. D., R. K. Mark, S. H. Cannon, and D. L. Knifong, Map of debris-flow hazard in the Honolulu District of Oahu, Hawaii, *U.S. Geol. Surv. Open File Rep.*, *93-213*, 25 pp., 1993.

Fowler, W. L., Potential debris flow hazards of the Big Bend drive drainage basin, Pacifica, California, Masters thesis, 101 pp., Dep. of Appl. Earth Sci., Stanford Univ., Stanford, Calif., 1984.

Hack, J. T., and J. C. Goodlet, Geomorphology and forest ecology of a mountain region in the central Appalachians, *U.S. Geol. Surv. Prof. Pap.*, *347*, 64 pp., 1960.

Hammond, C., D. Hall, S. Miller, and P. Swetik, Level 1 stability analysis (LISA) documentation for version 2.0, *Gen. Tech. Rep. INT-285*, 190 pp., U.S. Dep. of Agric., For. Serv., Intermountain Res. Stn., Ogden, Utah, 1992.

Hollingsworth, R., and G. S. Kovacs, Soil slumps and debris flows: Prediction and protection, *Bull. Assoc. Eng. Geol.*, *18*, 17–28, 1981.

Ikeya, H., A method for designation for areas in danger of debris flow, in Erosion and Sediment Transport in Pacific Rim Steeplands, *IAHS Spec. Publ.*, *132*, 576–588, 1981.

Iverson, R. M., and J. J. Major, Groundwater seepage vectors and the potential for hillslope failure and debris flow mobilization, *Water Resour. Res.*, *22*, 1543–1548, 1986.

Lehre, A. K., Sediment mobilization and production from a small mountain catchment: Lone Tree Creek, Marin county, California, Ph.D. dissertation, Dep. of Geol. and Geophys., Univ. of Calif., Berkeley, 1982.

Mark, R. K., Map of debris-flow probability, San Mateo County, California, scale 1:62,500, *U.S. Geol. Surv. Misc. Invest. Map*, *I-1257-M*, 1992.

Montgomery, D. R., Channel initiation and landscape evolution, Ph.D. dissertation, 421 pp., Dep. of Geol. and Geophys., Univ. of Calif., Berkeley, 1991.

Montgomery, D. R., and W. E. Dietrich, Where do channels begin?, *Nature*, *336*, 232–234, 1988.

Montgomery, D. R., and W. E. Dietrich, Source areas, drainage density, and channel initiation, *Water Resour. Res.*, *25*, 1907–1918, 1989.

Montgomery, D. R., and W. E. Dietrich, Channel initiation and the problem of landscape scale, *Science*, *255*, 826–830, 1992.

Montgomery, D. R., W. E. Dietrich, R. Torres, S. P. Anderson, J. T. Heffner, K. O. Sullivan, and K. Loague, Hydrologic experiments in a steep unchanneled valley, 1, Experimental design and piezometric response, *Eos Trans. AGU*, *71*, 1342, 1990.

Montgomery, D. R., R. H. Wright, and T. Booth, Debris flow hazard mitigation for colluvium-filled swales, *Bull. Assoc. Eng. Geol.*, *28*, 303–323, 1991.

Neely, M. K., and R. M. Rice, Estimating risk of debris slides after timber harvest in northwestern California, *Bull. Assoc. Eng. Geol.*, *27*, 281–289, 1990.

Neuland, H., A prediction model of landslips, *Catena*, *3*, 215–230, 1976.

Neuland, H., Diskriminanzanalytische untersuchungen zur identifikation der auslösefaktoren für rutschungen in verschiedenen höhenstufen der Kolumbianischen Anden, *Catena*, *7*, 205–221, 1980.

Okimura, T., and R. Ichikawa, A prediction method for surface failures by movements of infiltrated water in a surface soil layer, *Nat. Disaster Sci.*, *7*, 41–51, 1985.

Okimura, T., and M. Nakagawa, A method for predicting surface mountain slope failure with a digital landform model, *Shin Sabo*, *41*, 48–56, 1988.

Okunishi, K., and T. Iida, Evolution of hillslopes including landslides, *Trans. Jpn. Geomorphol. Union*, *2*, 191–200, 1983.

O'Loughlin, E. M., Prediction of surface saturation zones in natural catchments by topographic analysis, *Water Resour. Res.*, *22*, 794–804, 1986.

Pike, R. J., The geometric signature: Quantifying landslide-terrain types from digital elevation models, *Math. Geol.*, *20*, 491–511, 1988.

Reneau, S. L., and W. E. Dietrich, Size and location of colluvial landslides in a steep forested landscape, *IAHS Publ.*, *165*, 39–49, 1987a.

Reneau, S. L., and W. E. Dietrich, The importance of hollows in debris flow studies; examples from Marin County, California, in Debris Flows/Avalanches: Process, Recognition and Mitigation, edited by J. E. Costa and G. F. Wieczorek, *Rev. Eng. Geol.*, *7*, 165–180, 1987b.

Reneau, S. L., W. E. Dietrich, C. J. Wilson, and J. D. Rogers, Colluvial deposits and associated landslides in the northern San Francisco Bay area, California, USA, in *Proceedings of IVth International Symposium on Landslides*, pp. 425–430, International Society of Soil Mechanics and Foundation Engineering, Toronto, Ont., Canada, 1984.

Roth, R. A., Landslide susceptibility in San Mateo County, California, Masters thesis, 87 pp., Dep. of Appl. Earth Sci., Stanford Univ., Stanford, Calif., 1982.

Schlichte, K., Aerial photo interpretation of the failure history of the Huelsdonk Ridge/Hoh River area, report, 17 pp., Washington State Dep. of Nat. Resour., Olympia, 1991.

Schroeder, W. L., and J. V. Alto, Soil properties for slope stability analysis; Oregon and Washington coastal mountains, *For. Sci.*, *29*, 823–833, 1983.

Seeley, M. W., and D. O. West, Approach to geologic hazard zoning for regional planning, Inyo National Forest, California and Nevada, *Bull. Assoc. Eng. Geol.*, *27*, 23–35, 1990.

Sidle, R. C., A theoretical model of the effects of timber harvesting on slope stability, *Water Resour. Res.*, *28*, 1897–1910, 1992.

Smith, T. C., A method for mapping relative susceptibility to debris flows, with an example from San Mateo County, in Landslides, Floods, and Marine Effects of the Storm of January 3–5, 1982, in the San Francisco Bay Region, California, edited by S. D. Ellen and G. F. Wieczorek, *U.S. Geol. Surv. Prof. Pap.*, *1434*, 185–194, 1988.

Smith, T. C., and E. W. Hart, Landslides and related storm damage, January 1982, San Francisco Bay Region, *Calif. Geol.*, *35*, 139–152, 1982.

Tabor, R. W., and W. M. Cady, Geologic map of the Olympic Peninsula, Washington, scale 1:125,000, *U.S. Geol. Surv. Map*, *I-994*, 1978.

Takahashi, T., K. Ashida, and K. Sawai, Delineation of debris flow hazard areas, in Erosion and Sediment Transport in Pacific Rim Steeplands, *IAHS Publ.*, *132*, 589–603, 1981.

Torres, R., D. R. Montgomery, S. P. Anderson, W. E. Dietrich, and K. Loague, Hydrologic experiments in a steep unchanneled valley, 2, Characterization of unsaturated response, *Eos Trans. AGU*, *71*, 1342, 1990.

Tsukamoto, Y., T. Ohta, and H. Noguchi, Hydrological and geomorphological studies of debris slides on forested hillslopes in Japan, in Recent Developments in the Explanation and Prediction of Erosion and Sediment Yield, edited by D. E. Walling, *IAHS Publ.*, *137*, 89–98, 1982.

Warhaftig, C., Structure of the Marin Headlands Block, California: A progress report, in *Franciscan Geology of Northern California*, *Publ. 43*, edited by M. C. Blake, Jr., pp. 31–50, Society of Economic Paleontologists and Minerologists, Pacific Coast Section, Bakersfield, Calif., 1984.

Wilson, C. J., and W. E. Dietrich, The contribution of bedrock groundwater flow to storm runoff and high pore pressure development in hollows, *IAHS Publ.*, *165*, 49–59, 1987.

Wright, R. H., R. H. Campbell, and T. H. Nilsen, Preparation and use of isopleth maps of landslide deposits, *Geology*, *2*, 483–485, 1974.

Yee, C. S., and R. D. Harr, Influence of soil aggregation on slope stability in the Oregon Coast Ranges, *Environ. Geol.*, *1*, 367–377, 1977.

Zhang, W., and D. R. Montgomery, Digital elevation model grid size, landscape representation, and hydrological simulations, *Water Resour. Res.*, in press, 1994.

W. E. Dietrich, Department of Geology and Geophysics, University of California, Berkeley, CA 94720.

D. R. Montgomery, Quaternary Research Center, University of Washington, Seattle, WA 98195.

(Received January 25, 1993; revised October 13, 1993; accepted October 22, 1993.)